

Track reconstruction efficiency measurement using $e^+e^- \rightarrow \tau^+\tau^-$ events at Belle II

Laura Zani^{a,*}

^a*Aix Marseille Univ, CNRS/IN2P3, CPPM,
Marseille, France*

E-mail: zani@cppm.in2p3.fr

We present the Belle II track reconstruction efficiency and Monte Carlo efficiency correction factors using τ -pair events, in which one τ lepton decays leptonically ($\tau \rightarrow l\nu\nu$, $l = e, \mu$) while the other decays hadronically into three charged pions ($\tau \rightarrow 3\pi\nu + n\pi^0$). These measurements are performed using the e^+e^- collision data recorded during the 2019 data taking periods, corresponding to a total integrated luminosity of 8.8 fb^{-1} .

*40th International Conference on High Energy physics - ICHEP2020
July 28 - August 6, 2020
Prague, Czech Republic (virtual meeting)*

*Speaker

1. Introduction

The SuperKEKB accelerator is an electron-positron asymmetric energy collider located at the KEK laboratory in Tsukuba (Japan). It provides e^+e^- collisions at 10.58 GeV center-of-mass energy right at the peak of the $\Upsilon(4S)$ resonance, which are being recorded by the Belle II detector [1]. On June 21st 2020, SuperKEKB delivered the world's highest instantaneous luminosity achieving the peak value of $2.40 \times 10^{34} \text{ cm}^{-2} \text{ s}^{-1}$. By design, it is expected to reach a final instantaneous luminosity approximately thirty times higher than its predecessor KEKB, $6 \times 10^{35} \text{ cm}^{-2} \text{ s}^{-1}$, by applying the large crossing angle nano-beam scheme technique. So far the Belle II experiment has collected 74 fb^{-1} collision data since the beginning of so-called Phase 3 data taking in March 2019, after its first successful commissioning in 2018 (Phase 2), and the final goal is to accumulate a total integrated luminosity of 50 ab^{-1} .

The $e^+e^- \rightarrow \tau^+\tau^-$ process provides a good test-bed for the performance of Belle II track finding algorithms [2]. The cross section for τ -pair production is large and close to that of B meson pairs at the $\Upsilon(4S)$ resonance energy. In addition, the jet-like topology of τ decay products is suitable to study tracking performance in a low multiplicity but high-density track environment. Moreover, the τ -pair kinematics cover a wide track momentum range from 200 MeV up to around 3.5 GeV. These measurements are performed using the e^+e^- collision data recorded during the 2019a, 2019b and 2019c data taking periods, corresponding to a total integrated luminosity of 8.8 fb^{-1} .

2. Measurement strategy

The tracking efficiency is measured using a tag-and-probe method, similar to the one developed previously by the *BaBar* collaboration [3]. The method uses $e^+e^- \rightarrow \tau^+\tau^-$ events, where one tau lepton decays leptonically ($\tau \rightarrow \ell^\pm \nu_\ell \bar{\nu}_\tau$, $\ell = e, \mu$) while the other decays hadronically into three charged pions ($\tau \rightarrow 3\pi^\pm \nu_\tau + n\pi^0$). These decays will be referred to, hereafter, as the *1-prong* and *3-prong* τ -decays, respectively (and the process as 3×1 τ -pair event). According to the origin of the track from 1-prong τ -decay, two channels are defined, the electron (muon) channel where the 1-prong track originates from an electron (muon) ($\tau \rightarrow e(\mu)^\pm \nu_e \bar{\nu}_\tau$). There is a small contribution coming from hadronic decays ($\tau \rightarrow \pi^\pm \nu_\tau + n\pi^0$), where the charged pion passes either the electron or muon identification criteria. This accounts for 1.89% (6.36%) of the total signal yield in the electron (muon) channels. The tree-level Feynman diagram for the targeted process can be seen in Figure 1. Three good quality tracks with total charge ± 1 are used to *tag* τ -pair events. The existence of an additional track, the *probe* track, can be inferred from charge conservation. This allows us to measure the Belle II track finding efficiency by checking whether or not the probe track was reconstructed. The tracking efficiency ϵ_{track} is defined by

$$\epsilon_{track} \cdot A = \frac{N_4}{N_3 + N_4}, \quad (1)$$

where N_4 is the number of tagged events where all four tracks are found, while N_3 is the number of events where the probe track is not found, and A is a factor that takes into account the acceptance of the Belle II detector for the probe track. The N_4 and N_3 samples will be referred to, hereafter, as the 4- and 3-track samples, respectively. For physics analyses, it is essential to measure the tracking

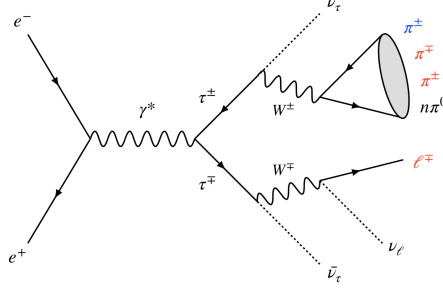


Figure 1: Feynman diagram for the $e^+e^- \rightarrow \tau^+\tau^-$ process targeted by the tag-and-probe method. The tag objects ($e^\mp \pi^\pm \pi^\mp$) are highlighted in red, while the probe pion is highlighted in blue.

efficiency in data to assign a systematic uncertainty for the mismodeling of the efficiency in Monte Carlo (MC) simulation. To this end, we define the data-MC discrepancy:

$$\delta = 1 - \frac{\epsilon_{\text{data}}}{\epsilon_{\text{MC}}}, \quad (2)$$

where ϵ_{data} and ϵ_{MC} are the tracking efficiencies measured in data and simulation, respectively. Simulated samples equivalent to a luminosity of 100 fb^{-1} are used for all signal and background processes, which include $\tau^+\tau^-$ events, $e^+e^- \rightarrow q\bar{q}$ continuum hadronization processes, low multiplicity final states and generic $B\bar{B}$ decays. When computing ϵ_{MC} the yields that enter Eq. 1 are from truth-matched signal according to the simulation, while for the ϵ_{data} computation the yields are the background subtracted data. The discrepancy estimator in Eq. 2 is calibrated (Sec. 4) and correction factors depending on the channel and charge of the final states are applied in order to correctly estimate the tracking efficiency discrepancy between simulation and data.

3. Event reconstruction and background suppression

Selected events in data are required to fire a hardware trigger line with a decision logic based on calorimeter information to provide an unbiased sample. Four lists of tracks are defined starting from a general good quality track list, selecting offline the tracks that come from the interaction point. Three classes of tag tracks that depend on whether they originate from a pion, electron or muon are provided. Regarding the fourth list for the probe track, a looser pion selection is also defined not to bias the efficiency measurement with tighter selections. Finally, depending on the channel and sample, events are required to satisfy different track multiplicity thresholds, but the total number of tracks in the event is unconstrained to prevent rejecting good events with additional beam-induced background tracks that do not pass any of the above mentioned selection lists. Note that the tag pion track selections are a subset of the probe pion selections. Due to the particle identification requirements, which exploit complementary selections on the ratio of the measured energy and momentum and the muon hypothesis likelihood, the electron and muon track lists are orthogonal to the others.

After requiring events to pass the trigger and track list requirements, there is still substantial background contamination coming mainly from the continuum ($e^+e^- \rightarrow q\bar{q}$, $q = u, d, s, c$), radiative

dilepton processes ($e^+e^- \rightarrow \ell^+\ell^-\gamma$, $\ell = e, \mu$) and $e^+e^- \rightarrow e^+e^-\mu^+\mu^-$. Additional selections are applied to suppress the background contributions. Hereafter, the two tag-tracks from the 3-prong τ -decay will be referred to as the 2-prong tracks. To exploit the signal-like event topology in rejecting combinatoric background we require that the 2-prong tracks and the probe have an angular separation from the 1-prong track of more than 120° in the center-of-mass system (CMS). Additionally, the 2-prong tracks are fitted to a common vertex and only good quality fit results are selected. Finally, to suppress the contamination from radiative QED and continuum hadronization processes the 1-prong track momentum normalized to the beam energy in the CMS is constrained to be within 0.2 and 0.8, as shown in Figure 2 (left); events are required to contain at most one π^0 and no more than two additional good photons; the opening angle between the 2-prong tracks in the electron (muon) channel is required to be greater than 0.2 (0.05) rad; the invariant mass of the tag tracks (M_{tag}) is required to be below 8.5 GeV (Figure 2, right); and the invariant mass of the 2-prong tracks ($M_{\pi\pi}$) is required to be below the τ lepton mass. After the previously mentioned selections, the remaining

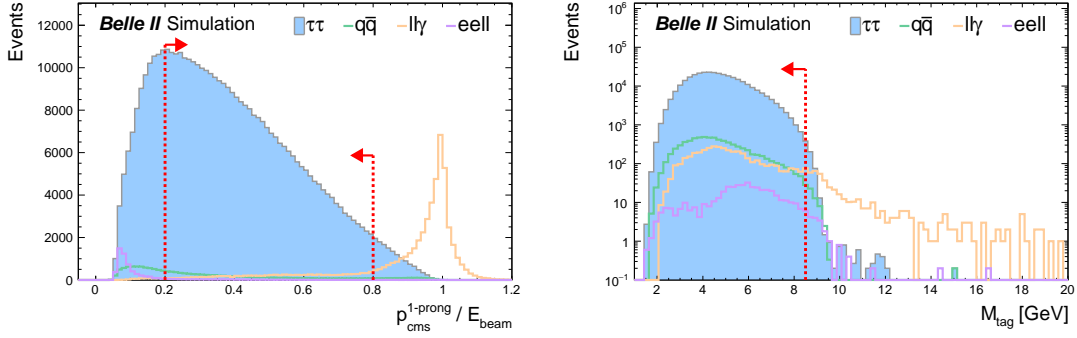


Figure 2: Distributions in MC simulation of the 1-prong track momentum divided by the beam energy (left) and the invariant mass of the reconstructed tag-track M_{tag} (right). The red arrows indicates the cut values.

contamination is apparently due to $ee\gamma^*$ events in the 3-track sample of the electron channel where the 2-prong tracks have opposite-sign charge (OS), whose reliable MC simulation is not available yet. Therefore, to reject this background we devise a data-driven veto. These events could mimic the signal-like final state topology if the positron is either not reconstructed or outside the detector acceptance. Such events are effectively suppressed in the electron-OS channel by requiring the missing mass squared is above 20 GeV^2 , and the polar angle of the missing momentum is between 40° and 135° . Here the missing quantities refer to the recoil system in the CMS frame with respect the reconstructed tag-tracks.

4. Data validation and calibration procedure

Data and simulation are compared after the final selections as a function of the 1-prong track transverse momentum in the laboratory frame and the invariant mass of the reconstructed tag tracks, as shown in the left and right plots of Figure 3, respectively. The simulation shows good agreement with data.

The discrepancy estimator defined in Eq. 2 is calibrated to represent the true value δ^* . The calibration is performed by introducing different known *per track* inefficiencies $\delta_{\text{MC}} =$

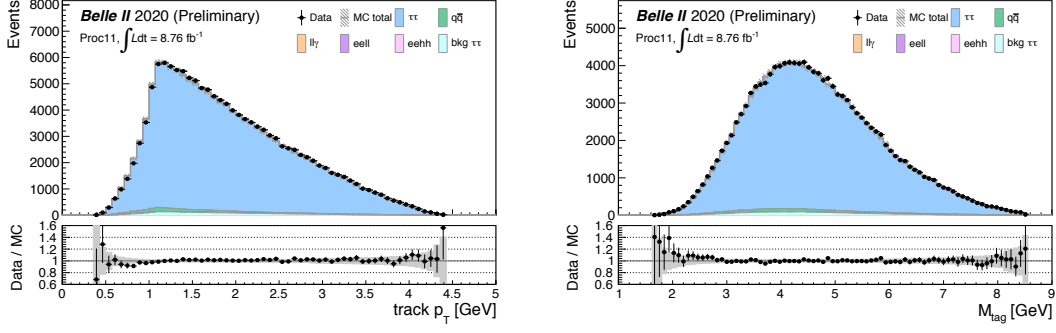


Figure 3: Distributions in data (black dots) and MC simulations (colored stacked histograms) of the 1-prong track transverse momentum in the laboratory frame (left) and the invariant mass of the reconstructed tag-track M_{tag} (right) are shown. MC samples are scaled to the total integrated data luminosity (8.8 fb^{-1}) and corrected bin-by-bin for the measured trigger efficiencies on data. The bottom plots show the bin-by-bin data to MC ratio, which is consistent with unity within the statistical uncertainty.

$\{2.5\%, 5\%, 7.5\%, 10\%\}$ in the simulated signal samples and applying the full analysis chain to extract the measured discrepancy δ_{meas} as done for the default simulation and data. The linear fit to the scatter plot of δ_{meas} measured on the modified signal simulations as a function of known inefficiencies δ_{MC} allows the extraction of the calibration factors k , which are reported in Figure 4. Therefore, the true value of the tracking efficiency discrepancy between data and simulation is

$$\delta^* = \frac{1}{k} \cdot \left(1 - \frac{\epsilon_{\text{data}}^{\text{meas}}}{\epsilon_{\text{MC}}^{\text{meas}}}\right).$$

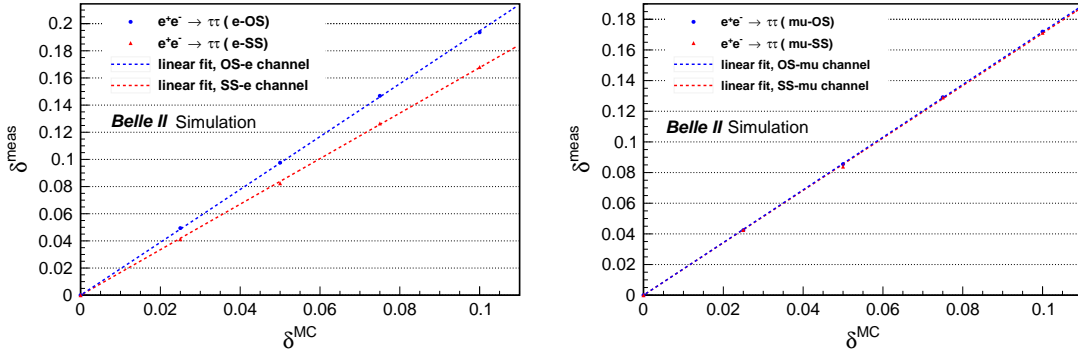


Figure 4: Calibration curves showing the measured discrepancy δ_{meas} as a function of the true one, δ_{MC} , for the electron (left) and muon (right) channels and for both charges OS (blue) and SS (red). The fit results provide the calibration curve slopes that correspond to the different calibration factors k : $k_{\text{OS}}^{\text{electron}} = 1.95 \pm 0.01$, $k_{\text{SS}}^{\text{electron}} = 1.68 \pm 0.01$, $k_{\text{OS}}^{\text{muon}} = 1.718 \pm 0.005$, $k_{\text{SS}}^{\text{muon}} = 1.709 \pm 0.008$.

5. Results

The efficiencies $\epsilon \times A$, computed as defined in Eq. 1, for data and simulation, as well as the calibrated discrepancies δ^* are shown in Figure 5. The latter are displayed for the different

channels and charges, both separately for each data taking period and combined. The overall combined data-MC discrepancy in the track finding efficiency, including the systematic uncertainty, is measured to be $\delta^* = 0.28 \pm 0.15(\text{stat}) \pm 0.73(\text{sys})\%$, where the uncertainty is dominated by the systematic contribution coming from the track charge dependence, which will be reduced once the charge-asymmetry effects are better understood.

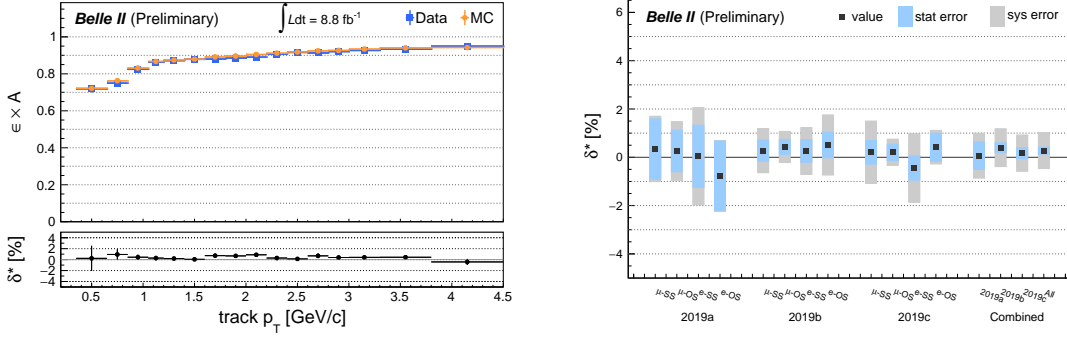


Figure 5: Measured tracking efficiency times detector acceptance $\epsilon \times A$ for the combined channels as a function of the 1-prong track p_T (left) and calibrated data-MC discrepancy δ^* (right) are shown. The upper panel in the left plot compares $\epsilon \times A$ in data (blue) and MC (orange), while the lower panel shows δ^* with statistical uncertainties only. In the right plot, the overall calibrated data-MC discrepancy as measured for the individual channels (μ -SS, μ -OS, e-SS, e-OS) as well as for the different data taking periods (2019a, 2019b, 2019c) is shown. The δ^* for the combined channels are shown in the rightmost four bins. Statistical (grey) and total systematic (blue) uncertainties are shown.

6. Conclusions

The Belle II experiment is taking data since the beginning of Phase 3 in March 2019. With the 8.8 fb^{-1} of data integrated during 2019 run periods, we devise an analysis strategy and calibration procedure that uses 3×1 decays in $\tau^+\tau^-$ events to measure the discrepancy in the track finding efficiency between data and simulation. The result is used to assign the systematic uncertainty related to tracking efficiency in physics analyses.

References

- [1] E. Kou *et al.* [Belle-II], PTEP **2019** (2019) no.12, 123C01 [erratum: PTEP **2020** (2020) no.2, 029201] doi:10.1093/ptep/ptz106 [arXiv:1808.10567 [hep-ex]].
- [2] V. Bertacchi *et al.* [Belle II Tracking], Comput. Phys. Commun. **259** (2021), 107610 doi:10.1016/j.cpc.2020.107610 [arXiv:2003.12466 [physics.ins-det]].
- [3] T. Allmendinger *et al.*, Nucl. Instrum. Meth. A **704** (2013), 44-59, doi:10.1016/j.nima.2012.11.184, [arXiv:1207.2849 [hep-ex]].